

Effect of deposition temperature on structural, microstructural and magnetic properties of CoFe_2O_4 thin films deposited by pulsed laser deposition

V. Madhav Kumar^{1,2} · A. Srinivas¹ · A. Talapatra³ · Saket Asthana² · J. Mohanty³ · S. V. Kamat¹

Received: 29 March 2016 / Accepted: 10 August 2016 / Published online: 20 October 2016
© Springer Science+Business Media New York 2016

Abstract A systematic study about the variation in microstructure and magnetic properties of Cobalt ferrite thin films, deposited on Si/SiO₂/TiO₂/Pt (111) substrate by using pulsed laser deposition at a constant oxygen pressure of 9 Pa with substrate temperatures ranging from 550 to 750 °C at an interval of 100 °C has been reported. All films showed the (111) preferred orientation with single phase confirmed by grazing incidence X-ray diffraction and Raman spectra. Moreover, the films showed all the active raman modes that were present in the cobalt ferrite target. The films deposited at 550 and 650 °C exhibits uniform and smooth surface features whereas deposition at 750 °C gives rise to porosities and voids due to re-evaporation of atoms from the deposited film. The grain size and roughness of the films increased with increasing deposition temperature. The induced in-plane tension in the film due to thermal expansion mismatch between substrate and film causes the increase in the perpendicular magnetic anisotropy. A sharp increase in out-of-plane coercivity and the domain size was observed at higher deposition temperatures.

1 Introduction

In recent years, cobalt ferrite thin film has acquired attraction because of its high coercivity, high magnetocrystalline anisotropy with higher chemical and mechanical stability. Moreover, it shows low conductivity and permeability (at higher frequencies), high magnetostriction coefficient and moderate saturation magnetization among cubic spinels. Due to these properties of cobalt ferrite, it can be used in many applications such as, magnetic sensors [1], magnetostrictive actuator [2], high-density recording media [3], magneto-optical devices [4], anode materials for Li-ion batteries [5] and microwave applications [6].

Cobalt ferrite has the inverse spinel structure with Fd3m space group and eight formula units ($8 \times 7 = 56$ ions) for a unit cell. In inverse spinel structures oxygen ions closely packed in FCC structure and there are two types of spaces available between these oxygen ions. One type of space will be available at the center of the tetrahedron in which corners of the tetrahedron are occupied by oxygen ions, called as tetrahedral site or A-site and the other type of space will be available at the center of the octahedron in which corners of the octahedron are occupied by oxygen ion, called as octahedral site or B-site. Out of 64 A sites 8 sites are occupied by 8Fe^{3+} ions and out of 32 B-sites 16 sites are occupied by 8Fe^{3+} and 8Co^{2+} ions in a random fashion [7].

Microstructure is one of the important properties in thin films. It can be tailored by growth conditions such as deposition temperature, pressure and also using substrates having different lattice parameters. In case of magnetic thin films, microstructure has its influence in magnetic properties, like magneto-crystalline anisotropy, coercivity and saturation magnetization [8]. Usually in films magneto-

✉ A. Srinivas
adirajs@dmrl.drdo.in

✉ Saket Asthana
asthanas@iith.ac.in

¹ Advanced Magnetics Group, Defence Metallurgical Research Laboratory, Kanchanbagh, Hyderabad 500058, India

² Advanced Functional Materials Laboratory, Department of Physics, Indian Institute of Technology Hyderabad, Sangareddy 502285, India

³ Nanomagnetism and Microscopy Laboratory, Department of Physics, Indian Institute of Technology Hyderabad, Sangareddy 502285, India

crystalline anisotropy and stress anisotropy play the key role. There are two types residual stresses that exist in films. First one is intrinsic which depends on deposition conditions. The other one is extrinsic residual stress, arises from the difference between thermal expansion coefficient of film and substrate [9].

Different research groups have studied the effect of substrate temperature on structural and magnetic properties of CFO films deposited on different substrates by using pulsed laser deposition (PLD) technique. Zhou et al. [10] reported that CFO films which were grown on Si (100) substrates as a function of the substrate temperature, ranging from 550 to 750 °C have the preferential orientation along <111> direction. For the (111) orientation, in-plane and out-of-plane coercivities of the CFO films increases with the substrate temperature. The rate of deposition was reported to be increasing up to a particular substrate temperature and thereafter it decreases. Dorsey et al. [11] stated that CFO films, grown on MgO (100) substrates at different substrate temperatures varying from 200 to 800 °C show (100) preferable orientation and the shift in diffraction peaks was observed as a function of substrate temperature. Coercivity values of CFO films were observed to be increasing along <100> direction with the increase in substrate temperature, but decrease along <001> and <011> directions. Magnetic anisotropy changes from uniaxial to a planar anisotropy as a function of substrate temperature. It is very clear from the literature that different substrates [12, 13] will drive the growth of the CFO films in different preferred orientation. Moreover, a re-orientation of anisotropy axis from in-plane to out-of-plane of the sample is also associated with increasing substrate temperature. Raghunathan et al. [12] studied various properties of the CFO films deposited on SiO₂/Si(100) substrates at different substrate temperatures ranging from 250 to 600 °C. The preferred orientation of the CFO films changed from (111) direction to (100) direction with the increase in substrate temperature. Perpendicular magnetic anisotropy, grain size and magnetic feature size increase with increasing deposition temperature, whereas in-plane magnetic anisotropy decreases with increase in deposition temperature. Thanga et al. [13] reported that the cobalt ferrite films on TiO₂-terminated (001) SrTiO₃ substrates as a function of substrate temperatures, varying from 500 to 700 °C exhibits epitaxial growth. At lower temperatures films shown smooth surface and in-plane magnetic anisotropy whereas at higher temperatures the in-plane magnetic anisotropy is less pronounced and film surface becomes rougher due to presence of particulates.

In this present study, we have investigated the role of deposition temperature on structural and magnetic properties of the CFO films deposited on Pt (111) substrate. Since Pt (111) substrate can be used as a bottom electrode while

doing the electric properties measurements and also it has advantages such as high electrical conductivity and stability in high-temperature oxidizing environments [14], so it is important to optimize and understand the deposition temperature effect on microstructural and magnetic properties of CFO films deposited on the Pt substrate.

2 Experimental procedure

Cobalt ferrite target was prepared by conventional solid state sintering route. Initially, Fe₂O₃ and Co₃O₄ were taken as the precursors in the stoichiometric ratios. The precursors were ball-milled for 2 h for uniform mixing and then calcined at 600 °C for 2 h. Finally, it is sintered at 1250 °C for 5 h. Cobalt ferrite films were deposited on Si/SiO₂/TiO₂/Pt (111) (Pt = 150 nm, TiO₂ = 50 nm, SiO₂ = 300 nm, Si = 0.5245 mm) substrate from the cobalt ferrite target by pulsed laser deposition technique (PLD) using a KrF excimer laser (248 nm) at laser energy 250 mJ with repetition rate of 10 Hz. Before deposition, substrate was ultrasonicated using acetone and methanol. During the deposition, target to substrate distance was kept fixed at 4 cm. To ensure the uniform deposition and stoichiometry in the films, target was allowed to rotate continuously across the laser beam [15]. By maintaining 9 Pa constant background oxygen pressure a series of three different deposition temperatures: i.e., 550, 650, 750 °C were investigated with same deposition time of 45 min. Prior to deposition, the chamber was pumped down to 2.7×10^{-4} Pa. After deposition, the films were cooled down to room temperature under the same background oxygen pressure at the rate of about 5 °C/min.

Phase formation and crystal structure of the CFO films were determined by grazing incidence X-ray diffraction (GI-XRD) Bruker (model: D8 discover) with Cu-K_α radiation ($\lambda = 1.5406$ Å). For further confirmation about phase, Raman spectra of the CFO films were recorded with Laser Raman spectrometer (Bruker, Senterra). The experiments were carried out at room temperature with an excitation source of wavelength 785 nm. Microstructures and cross-section of the films were observed from the field emission scanning electron microscopy (FESEM) (model: Carl Zeiss, Supra 40). Field dependent magnetization values of the films were measured at room temperature with super conducting quantum interference device (SQUID) magnetometer (Quantum Design, MPMS-5T) by applying magnetic field along the parallel (in-plane) and perpendicular (out-of-plane) to the film surface. Roughness and surface morphologies of the deposited films were examined by Atomic Force Microscopy (AFM). The domains width and orientation of the domains in the films were determined

by using Magnetic Force Microscopy (MFM) (model: Bruker, dimension icon).

3 Results and discussion

Figure 1 shows the X-ray diffraction patterns of the CFO films deposited at 550, 650, and 750 °C and these patterns are indicating that all CFO films are stabilized in single phase pure CoFe_2O_4 with $\text{Fd}\bar{3}m$ space group and the films showed diffraction peaks corresponding to (311), (511) and (400) planes (JCPDS PDF No. 221086) of cubic structure of spinel system. The higher intensity of the (311) and (511) peaks reveal that the film is textured along (111) direction. Intensity of (400) peak enhances with increase in deposition temperature. With the increasing deposition temperature the major intense peaks {(311), (511) and (400)} in the X-ray diffraction getting sharper which is related to enhancement of the grain size of the deposited films.

Factor group analysis predicts the following phonon modes for the spinel structure: $A_{1g}(\text{R}) + E_g(\text{R}) + T_{1g} + 3T_{2g}(\text{R}) + 2A_{2u} + 2E_u + 4T_{1u}(\text{IR}) + 2T_{2u}$. Out of these phonon modes five are Raman active modes, namely A_{1g} , E_g and $3T_{2g}$. As indicated in the Fig. 2a, b, the CFO target showed the Raman modes at 180, 308, 472, 562, 618 and 684 cm^{-1} and CFO films also showed the all Raman modes at the same frequency as CFO target with change in the intensity. This confirms the formation of single phase CFO films deposited at different substrate temperature. The Raman modes at above 600 cm^{-1} corresponds to the symmetric stretching of oxygen atom with respect to the metal ion in tetrahedral void, tetrahedral breath mode and is assigned as A_{1g} . The other low frequency modes corresponds to symmetric and anti-symmetric bending of oxygen atom in metal-ion (M–O) bond at octahedral voids and

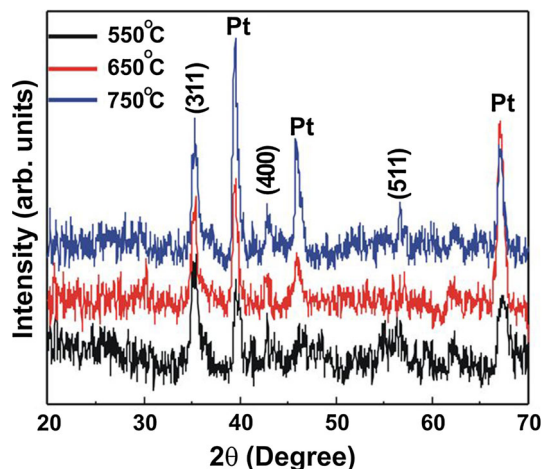


Fig. 1 X-ray diffraction patterns of CFO films deposited at 550, 650 and 750 °C

assigned them as E_g and (3) T_{2g} . All modes are assigned according to literature [16]. In order to estimate the ratio of Co^{2+} ions at the tetrahedral site and octahedral site, we calculated the intensity ratio of the peaks corresponding to the tetrahedral (618 cm^{-1}) site [16] and octahedral (472 cm^{-1}) site [17]. As displayed in the Fig. 2c, the peak intensity ratio rises with increasing of the deposition temperature which specifies that some of the Co^{2+} ions shift from octahedral sites to tetrahedral sites with the effect of higher deposition temperature. This result is similar to the observation made (according to crystal field theory) by Sharma and Khare [18], studied with increasing annealing temperature.

Figure 3a–c, depicts the surface FESEM micrographs of the deposited CFO films. The grain size of the CFO films increased from 40 to 100 nm with increasing the deposition temperature from 550 to 750 °C. For the films deposited at 550 °C, the grains may not be fully grown due to insufficient thermal energy and for films deposited at 650 °C shows uniform and smooth features. Interestingly the films deposited at 750 °C shows the flakes type of grain structure but films have the more porosity and voids when compared with other films. Usually the film growth (nucleation) rate on a substrate consists of several processes such as arrival of film atoms on bare substrate areas or pre-existing cluster surface. Diffusion of these atoms over the substrate surface or cluster surface will construct mobile or stationary clusters, diffusion of atoms to cluster or dissociation of atoms from cluster, re-evaporation of atoms from cluster or substrate. The balance between growth and dissolution processes for a given cluster will be governed by the total free energy of the cluster, relative to the assembly of individual atoms. The total free energy can be written as

$$\Delta G = a_1 r^2 \Gamma_{c-v} + a_2 r^2 \Gamma_{s-c} - a_2 r^2 \Gamma_{s-v} + a_3 r^3 \Delta G_v$$

where r is the radius of the cluster, Γ are the interface energies, a 's are constants that depend on the shape of the nuclei and ΔG_v is the change in volume free energy on condensation of the cluster. For a given cluster, if the derivative of the free-energy change with respect to atom in cluster is positive, then the cluster is not stable and will shrink on average. If the derivative is negative, then the size of cluster is stable and will grow on average. The volume free-energy will become more negative for increased supersaturation of vapor atoms on the surface and supersaturation will increase with the decrease in the substrate temperature. Hence in practice, we do make free-energy change more negative by decreasing the substrate temperature. An increase in the magnitude of the negative volume free energy will increase the cluster nucleation rate. A decrease of substrate temperature will also give rise to decrease the surface diffusion coefficient of the adsorbed vapor atoms. The competition between increased

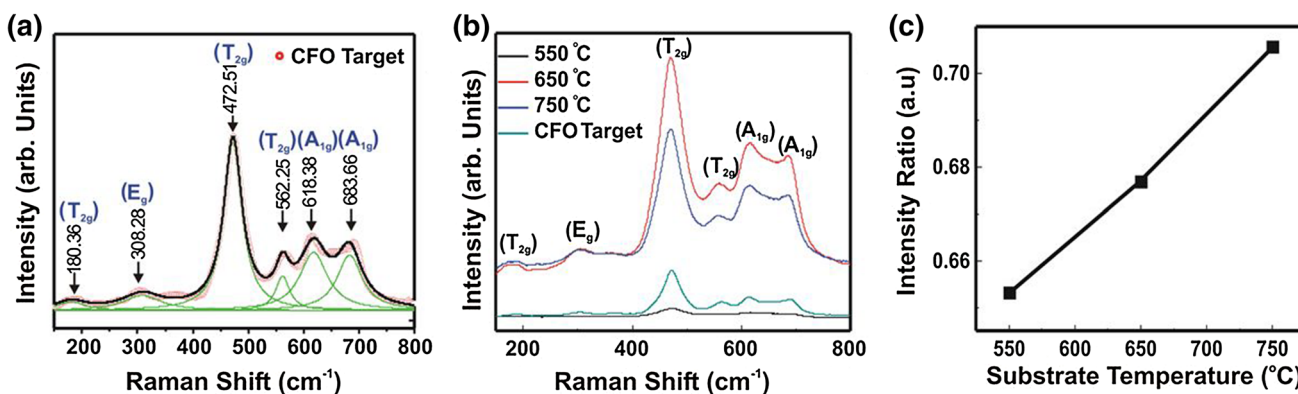


Fig. 2 Room temperature Raman spectra of **a** CFO target, **b** CFO films deposited at 550, 650 and 750 °C, **c** variation of intensity ratio of Raman peaks at 618 and 472 cm^{-1} with variation of deposition temperature

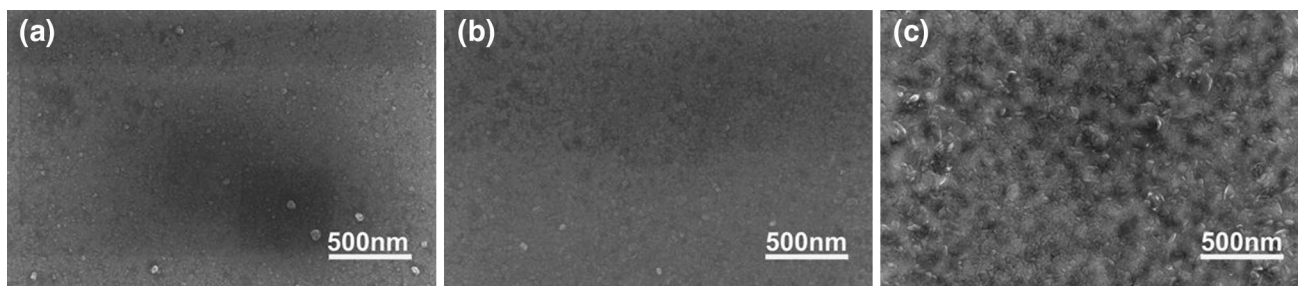


Fig. 3 FESEM surface micrographs of CFO films deposited at **a** 550 °C, **b** 650 °C, **c** 750 °C

supersaturation and decreased diffusion coefficient with decreasing the substrate temperature leads to a maximum nucleation rate at certain temperature and decreased nucleation rate above and below that temperature [19].

Figure 4a–c displays the cross sectional images of the CFO films. As shown here, except the film deposited at 550 °C, all the films exhibited uniform deposition throughout the film and the films are well attached to the substrate. The thickness of the films increases from 247 to 290 nm with increasing the deposition temperature from 550 to 750 °C indicating that deposition rate increases with the substrate temperature as shown in Table 1. Even though the deposition rate is high for the film deposited at 750 °C due to re-evaporation of atoms from the film, it contains more porosities and voids. Small amount of the film

Table 1 Results from the FESEM micrographs and cross sectional images

Deposition temperature (°C)	Grain size (nm)	Thickness (nm)
550	40	247
650	67	267
750	100	290

diffuses into the substrate for the films deposited at 750 °C. On the other hand the films deposited 650 °C has the uniform thickness throughout the film. In addition, there is a gradual increase of grain size as shown in Table 1.

Now, in order to estimate the magnetic properties of the films, room temperature hysteresis loops (M–H loops) are

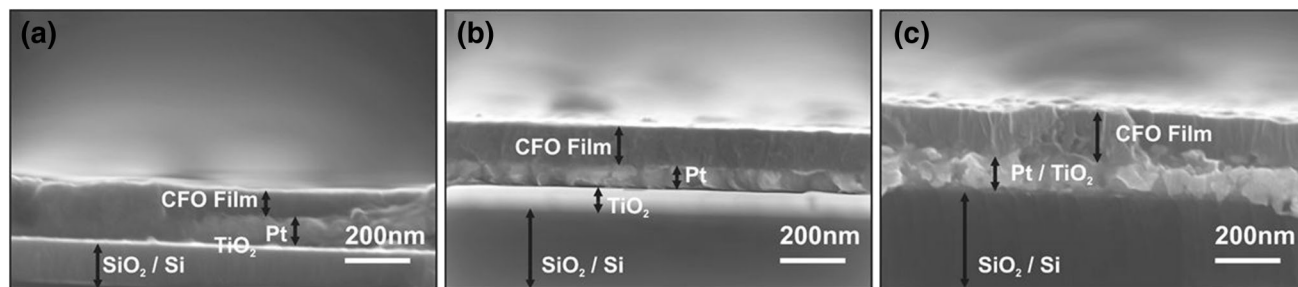


Fig. 4 FESEM cross-sectional images of CFO films deposited at **a** 550 °C, **b** 650 °C, **c** 750 °C

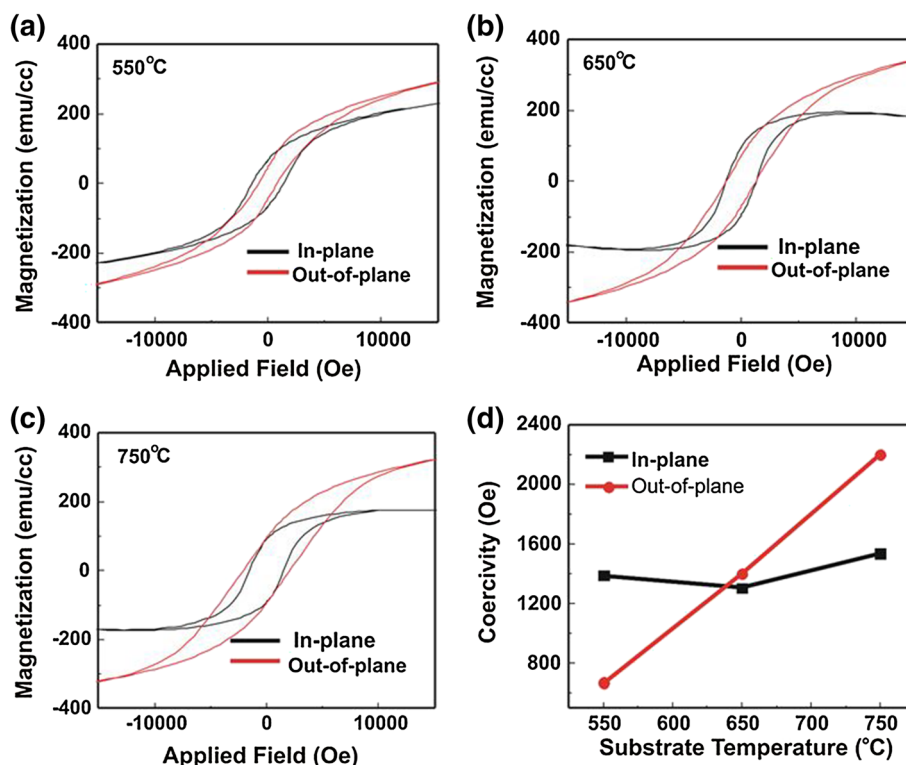
measured with applying external magnetic field along the plane and out of the plane with respect to the sample surface as shown in Fig. 5a–c for the films deposited at 550, 650, and 750 °C respectively. There is no significant variation in the in-plane coercivity with the increase in substrate temperature while the out-of-plane coercivity has increased with increasing substrate temperature. As shown in the Fig. 5a–c the films which were deposited at lower temperature (550 °C), exhibits more in-plane coercivity and the films deposited at 650 °C show nearly equal value of in-plane and out-of-plane coercivity but the films deposited at 750 °C exhibits a large out-of-plane coercivity compared to the in-plane one. The CFO films shown (111) preferred orientation because the closed-packed {111} planes of spinel ferrites have the lowest surface energy which makes the energetically favorable {111} oriented spinel surfaces [20]. According to the magnetocrystalline anisotropy theories, the direction $\langle 111 \rangle$ is the direction of easy magnetization in all the cubic ferrites, except cobalt ferrite or mixed ferrites containing a large amount of cobalt which has $\langle 100 \rangle$ direction as the direction of easy axis of magnetization and $\langle 111 \rangle$ direction as hard axis of magnetization [10]. The direction of easy magnetization of a crystal is the direction of spontaneous domain magnetization in the demagnetized state, hence in the demagnetized state, the magnetic moments are favorable to be in the plane of the surface. Therefore, the films deposited at lower

temperatures are exhibiting more in-plane coercivity. As shown in the Fig. 5f, the out-of-plane coercivity rises with increase in the substrate temperature. Thermal expansion coefficient of Platinum and CFO are reported 9×10^{-6} and $14.9 \times 10^{-6} \text{ } ^\circ\text{C}^{-1}$ respectively [21, 22]. Due to this mismatch, an in-plane isotropic tension will be induced in the film during the cooling process of the substrate-film combination from deposition temperature to room temperature. The amount of strain induced in the film due to the mismatch in thermal expansion coefficient of film and substrate can be calculated from the formula given as [23]:

$$\varepsilon = (\alpha_s - \alpha_f)\Delta T$$

where ΔT is the difference between the deposition temperature and the measuring temperature. α_s and α_f are the thermal expansion coefficients of substrate and film respectively. Since CFO has a negative magnetostriction (10), in-plane isotropic tension expected to give rise to the perpendicular magnetic anisotropy, hence increases in deposition temperature leads to an increment in the amount of strain induced in the film which results in enhancement of the out-of-plane coercivity. Apart from induced strain, (grain size also will affect the coercivity) or coercivity will also depend on the grain size [24]. As shown in the Fig. 3a–c with the increase in grain size, the coercivity of the system also increases (Fig. 5a–c) due to the increase in magnetic anisotropy energy ($K_u \times V$). Due to this, thermal

Fig. 5 M-H loops measured at in-plane and out-of-plane geometries for CFO films deposited at substrate temperature **a** 550 °C, **b** 650 °C, **c** 750 °C, **d** Variation of coercivity with substrate temperature



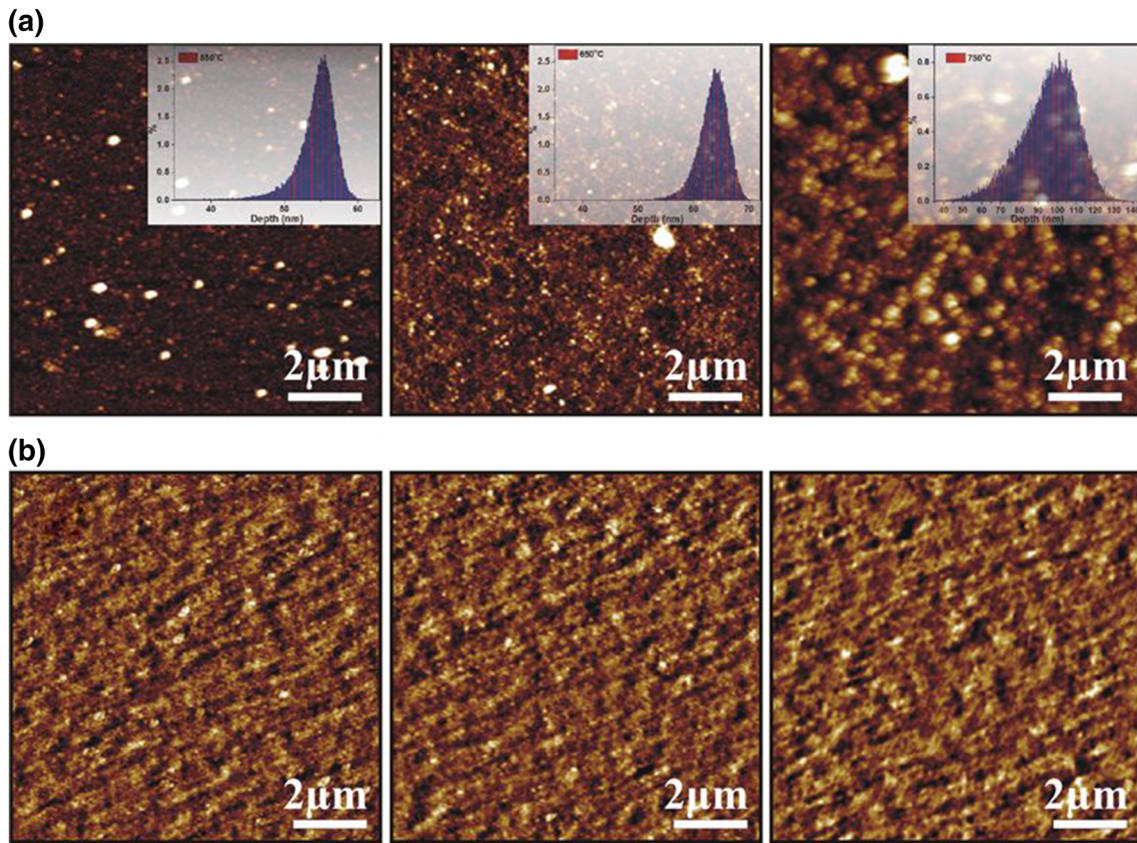


Fig. 6 **a** AFM with depth histogram as inset and **b** MFM images for CFO films deposited at substrate temperature 550, 650 and 750 °C (from left to right)

Table 2 Results from the AFM and MFM images

Deposition temperature(°C)	Roughness (nm)	Threshold height (nm)	Domain size (nm)
550	4	54	150
650	3	64	208
750	16	101	221

energy becomes less effective to change the magnetization and more external field is required for magnetization reversal. Hence, coercivity increases. This is true when the grain size is smaller than the domain size, as in our case [25].

Atomic force microscopy (AFM) is carried out for all the three CFO films deposited at 550, 650 and 750 °C. For the first two films, roughness comes about 4 and 3 nm, but for the third one roughness increases to 16 nm and a particulate feature is observed in the topography image. We have calculated the depth histogram which indicates the particle size distribution over the entire area of scan. This shows the threshold heights are almost 54, 64 and 101 nm for our three films deposited at 550, 650, and 750 °C respectively. These values are also comparable to the grain sizes as obtained from FESEM images. To check the domain structure [26] in our films, we have performed

magnetic force microscopy (MFM) at room temperature without application of external magnetic field. Formation of domains in magnetic materials is the result of minimization of competitive energies of the system due to magnetostatic interaction between spins, anisotropy, exchange coupling and Zeeman energy due to external magnetic field and magneto-elastic interactions [7]. For thin films, the correlation between magnetostatic energy and anisotropy energy decides the domain formation. The effective anisotropy (k_{ef}) of the film is the addition of volume and surface anisotropy. With the increase in thickness, the volume anisotropy gets enhanced and when it is comparable to the surface anisotropy, the system breaks into domains. In this situation, magnetostatic energy due to flux closure is high enough to support the domain formation. With MFM, we probe the films with a magnetized tip, having a fixed lift height (30 nm in our

experiment) from the surface of the film. Our MFM images (Fig. 6b) show the existence of magnetic domains having two different contrasts. As MFM is sensitive to the out-of-plane signal from the material and useful to image the magnetic state at equilibrium [27], so two different contrasts basically designate the magnetization parallel or anti-parallel to the surface normal. The domain size is measured by performing line scan over the domains at different locations and is observed to be increasing around 48 % when the deposition temperature was varied from 550 to 750 °C. Increase in thickness due to higher deposition rate at higher temperature may result to this effect [28]. But the orientation of the domains does not change. A systematic study with temperature and field dependent MFM [29] will surely throw light over the orientation of anisotropy axis and possible spin-reorientation in the material with varying deposition temperature, which is our future goal. The results obtained from the AFM and MFM studies are depicted in Table 2.

4 Conclusions

We have performed the study of microstructure and magnetic properties for CFO thin films deposited by PLD technique. The films, grown over Si/SiO₂/TiO₂/Pt (111) substrates with background oxygen pressure of 9 Pa showed (111) preferred orientation and the major intensity peaks become sharper with the increase in substrate temperature. Raman spectra of the CFO films displayed all modes as observed for the CFO target. Films deposited at 550 and 650 °C exhibit uniform and smooth surface whereas the film deposited at 750 °C showed more porosities and voids. Moreover, the cross-sectional FESEM study showed higher film thickness at elevated temperature due to the higher growth rate. The films show higher values of grain size at higher deposition temperature. Depth histogram analysis of the AFM images reveals that the particle size distribution over the scanned area gets broadened along with the increase in threshold height nearly by 50 % for the films deposited at 750 °C compared to that of 550 °C. From the results of the M–H loops, it is evident that the out-of-plane coercivity sharply increases with deposition temperature whereas the change in in-plane coercivity is not that significant. The variation in domain size also follows the similar trend as that of out-of-plane coercivity. MFM being very sensitive to the out-of-plane signal from the magnetic material, an indication about the growth of perpendicular anisotropy is observed for the films, deposited at higher temperatures. This can be attributed to the mismatch of thermal expansion coefficients between the film and the substrate which results in

an in-plane isotropic tension induced in the film at higher deposition temperature. An indication of increase in perpendicular magnetic anisotropy is observed as the perpendicular coercivity and the domain size show increasing trend at higher deposition temperature. Future study with films having same thickness, deposited at different temperature along with extensive microscopy can throw light to the proper spin re-orientation in CFO thin films.

Acknowledgments Authors V. Madhav Kumar, Saket Asthana and A. Srinivas are thankful to Defence Research and Development Organization (DRDO) for their funding to carry out this work under the Grant No. ERIP/ER/1100415/M/01/1430, Government of India.

References

1. J.A. Paulsen, A.P. Ring, C.C.H. Lo, J.E. Snyder, D.C. Jiles, J. Appl. Phys. **97**, 044502 (2005)
2. D.C. Jiles, J. Phys. D **28**, 1537–1546 (1995)
3. A.K. Giri, E.M. Kirkpatrick, P. Moongkhamklang, S.A. Majetich, V.G. Harris, Appl. Phys. Lett. **80**, 2341 (2002)
4. S.N. Okuno, S. Hashimoto, K. Inomata, J. Appl. Phys. **71**, 5926 (1992)
5. Y.Q. Chu, Z.W. Fu, Q.Z. Qin, Electrochim. Acta **49**, 4915–4921 (2004)
6. Z. Su, S. Bennett, B. Hu, Y. Chen, V.G. Harris, J. Appl. Phys. **115**, 17A504 (2014)
7. B.D. Cullity, C.D. Graham, *Introduction to Magnetic Materials*, 2nd edn. (Wiley, New Jersey, 2009)
8. G. Hu, J.H. Choi, C.B. Eom, V.G. Harris, Y. Suzuki, Phys. Rev. B **62**, R779–R782 (2000)
9. M. Khodaei, S.A.S. Ebrahimi, Y.J. Park, J.M. Ok, J.S. Kim, J. Son, S. Baik, J. Magn. Mater. **340**, 16–22 (2013)
10. J.P. Zhou, H.C. He, C.W. Nan, Appl. Surf. Sci. **253**, 7456–7460 (2007)
11. P.C. Dorsey, P. Lubitz, D.B. Chrisey, J.S. Horwitz, J. Appl. Phys. **79**, 6338 (1996)
12. A. Raghunathan, I.C. Nlebedim, D.C. Jiles, J.E. Snyder, J. Appl. Phys. **107**, 09A516 (2010)
13. P.D. Thanga, G. Rijnders, D.H.A. Blanka, J. Magn. Mater. **310**, 2621–2623 (2007)
14. M.L. Yi, C.B. Wang, Q. Shen, L.M. Zhang, J. Mater. Sci.: Mater. Electron. **25**, 82–86 (2014)
15. J.P. Zhou, H.C. He, C.W. Nan, Appl. Surf. Sci. **253**, 7456–7460 (2007)
16. P. Chandramohan, M.P. Srinivasan, S. Velmurugan, S.V. Narasimhan, J. Solid State Chem. **184**, 89–96 (2011)
17. X. Fan, J. Guan, X. Cao, W. Wang, F. Mou, Eur. J. Inorg. Chem. **2010**, 419–426 (2010)
18. D. Sharma, N. Khare, Appl. Phys. Lett. **105**, 032404 (2014)
19. D.B. Chrisey, G.K. Hubler, *Pulsed Laser Deposition of Thin Films*, 1st edn. (Wiley-Interscience Publication, New York, 1994)
20. K. Raja, Mishra and G. Thomas. J. Appl. Phys. **48**, 4576 (1977)
21. R.E. Tylor et al., *Thermal Expansion of Solids* (ASM International, Russell Township, 1998)
22. N. Li, Y.-H.A. Wang, M.N. Iliev, T.M. Klein, A. Gupta, Chem. Vap. Depos. **17**, 261 (2011)
23. M. Ohring, *Material Science of Thin Films*, 2nd edn. (Academic Press, Cambridge, 2002)
24. J. Yin, J. Ding, B. Liu, Y. Wang, J. Yi, J. Chen, X. Miao, IEEE Trans. Magn. **41**, 3904–3906 (2005)

25. Y. Jianhua, Deposition, *Microstructure and Magnetic anisotropy of Cobalt Ferrite Thin Films* (Data Storage Institute, Department of Material Science, National University of Singapore, 2008)
26. O. Hellwig, J.B. Kortright, A. Berger, E.E. Fullerton, J. Magn. Mater. **13**, 319 (2007)
27. A. Talapatra, J. Mohanty, J. Magn. Mater. (2016). doi:[10.1016/j.jmmm.2016.02.051](https://doi.org/10.1016/j.jmmm.2016.02.051)
28. A. Talapatra, J. Mohanty, AIP Conf. Proc. **1731**, 130027 (2016)
29. J. Mohanty, R. Engel-Herbert, T. Hesjedal, Appl. Phys. A **81**, 1359–1362 (2005)